Infrared and Raman Spectra, Conformational Stability, Ab Initio Calculations, and Vibrational Assignment of 1-Penten-4-yne†

James R. Durig,* Xiaodong Zhu,‡ and Gamil A. Guirgis

Department of Chemistry, University of Missouri−Kansas City, Kansas City, Missouri 64110-2499

Frederick J. Heldrich and Matthew J. Wright

Department of Chemistry and Biochemistry, College of Charleston, Charleston, South Carolina 29403

Received: December 31, 2002; In Final Form: April 9, 2003

The infrared spectra (3500−50 cm^{-1}) of gas and solid and the Raman spectra (3500−50 cm^{-1}) of liquid and solid 1-penten-4-yne, CH_2═$CHCH_2C$≡CH, have been recorded. Variable-temperature studies over the range −105 to −150 °C of the infrared spectra (3500−400 cm^{-1}) of the sample dissolved in liquid krypton have also been recorded. By utilizing the relative intensities of five syn/gauche conformer pairs, the syn conformer is found to be the lower energy form with an enthalpy difference of 248 ± 25 cm^{-1} (2.97 ± 0.30 kJ/mol). At ambient temperature it is estimated that there is 38% ± 2% of the gauche conformer present. Equilibrium geometries and total energies of the two conformers have been determined from ab initio calculations with full electron correlation by the perturbation method to second order as well as by hybrid density functional theory (DFT) calculation with the B3LYP method using a number of basis sets. The smaller basis sets with diffuse functions predict the gauche conformer to be the more stable form, whereas other calculations predict the syn conformer to be the lower energy rotamer. The B3LYP calculations predict a much lower energy difference between the conformers than found experimentally. A complete vibrational assignment is proposed for the syn conformer and many of the fundamentals have been identified for the gauche form on the basis of the force constants, relative intensities, and depolarization ratios obtained from MP2/6-31(d) ab initio calculations as well as on rotational−vibrational band contours obtained from the predicted equilibrium geometric parameters. The r_0 structural parameters are estimated for 1-penten-4-yne from ab initio MP2/6-311+G(d,p) calculations, and comparisons are made with those of allyl fluoride and cyanide. The spectroscopic and theoretical results are compared to the corresponding properties for some similar molecules.

Introduction

The structural parameters, conformational stability, and vibrational spectra of the 3-monosubstituted propenes, CH_2═$CHCH_2X$, where X = F,[1,2] Cl,[3] Br,[4,5] I,[6] CN,[7] CH_3,[8] SiH_3,[9] NH_2,[10−13] OH,[14,15] etc., have been of interest for several years. For the 3-halopropenes (allyl halides) only the fluoride has the syn conformer as the more stable rotamer, but many of the ab initio calculations[16] at the MP2 level with full electron correlation utilizing relatively large basis sets with diffuse functions predict the gauche conformer as the more stable form. Similar problems also exist for the prediction of the conformational stability of 1-butene[8] (X = CH_3) but not for 3-cyanopropene,[7] CH_2═$CHCH_2CN$, where the experimental enthalpy difference is 336 cm^{-1}. Since the ethynyl group, C≡C−H, has an electronegativity similar to that of the cyano group,[17] we initiated a vibrational spectroscopic and theoretical investigation of the conformational stability of 1-penten-4-yne, CH_2═$CHCH_2C$≡CH.

There have been no previous vibrational studies reported for 1-penten-4-yne, and we therefore recorded the Raman spectra of the liquid and solid along with the infrared spectra of the gas, krypton solutions with variable temperatures, and the solid. We have also carried out ab initio calculations employing the 6-31G(d) basis set at the level of restricted Hartree−Fock (RHF) and with the Møller−Plesset perturbation method to the second order (MP2) to obtain equilibrium geometries, force constants, vibrational frequencies, infrared and Raman intensities, and conformational stabilities. Structural parameters and conformational stabilities have also been obtained from the larger basis sets of 6-311+G(d,p) and 6-311+G(2d,2p) as well as without diffuse functions at the MP2 level with full electron correlation. Density functional theory (DFT) calculations by the B3LYP method with a variety of basis sets have also been carried out. The results of this spectroscopic and theoretical study are reported herein.

Experimental Section

The 1-penten-4-yne sample was prepared by modification of a Grignard coupling procedure.[18] A multiple-neck, 2-L, round-bottom flask fit with a condenser, septum, and magnetic stir bar was flame-dried under positive Ar. To the flask was added 1.2 L (0.60 mol) of commercially available ethynylmagnesium bromide [0.5 M in tetrahydrofuran (THF)] and 4.55 g (0.02 mol) of CuBr·dimethyl sulfide. The suspension was stirred at room temperature for 20 min and then 46 mL (0.53 mol) of allyl bromide was poured into the reaction vessel. The reactants gradually warmed and self-refluxed within 5 min, after which

† Part of the special issue "A. C. Albrecht Memorial Issue".

* Corresponding author: phone 01 816-235-6083; fax 01 816-235-2290; e-mail durigj@umkc.edu.

‡ Taken in part from the thesis of X.Z., which will be submitted to the Department of Chemistry in partial fulfillment of the Ph.D. degree.

10.1021/jp022649r CCC: $25.00
Published on Web 06/03/2003

time the solution was maintained at reflux for an additional 2 h and then allowed to stir overnight at room temperature under positive Ar pressure. The resulting thick slurry was treated with 1 L of pH 5 buffer solution and 1 L of water and then split into two portions of equal volume. Each portion was treated equally by extraction with Decalin in four 200 mL portions. The Decalin extracts were then washed with water (2 × 300 mL). An emulsion layer, formed during the extractions, was set aside and treated separately. To the combined emulsions (800 mL) were added brine (500 mL) and water (1.5 L). The organic layer that separated was isolated and then washed with additional water (1 L). The combined organics were then washed with water (15 × 500 mL), followed with brine (2 × 300 mL), and then dried over anhydrous Na_2SO_4, filtered, and fractionally distilled through a 10-cm column of glass Raschig rings. The distillate, with boiling point up to 65 °C, was collected. Gas chromatography (GC) analysis indicated a distillate composition of approximately 1:1 product and THF. The distillate mixture was washed with water (12 × 40 mL), at which point GC indicated that no THF remained. This material was dried neat with Na_2SO_4, filtered, and subjected to a simple distillation to yield 8.58 g (0.13 mol) of the product (bp 41−47 °C, uncorrected, 8.58 g, 0.13 mol, 24.5%).

Routine characterization by IR, MS, and NMR confirmed the product's structure and were obtained by a Mattson-Genesis II Fourier transform infrared (FT-IR) instrument with the Golden Gate accessory (diamond cell for liquid solutions, or solids). Routine MS data were recorded on a Hewlett-Packard 5971 MSD; *m/e* (relative intensity) 67 (4.9%), 66 (100%), 39 (42.6%). Routine ^{1}H NMR[19] spectra were recorded in $CDCl_3$ at 300 MHz on a Varian Mercury system; ppm (m, *J*, no. of H) 5.83 (d of d of t, $J_{trans} = 17$ Hz, $J_{syn} = 10$ Hz, $J_{2-3} = 5.3$ Hz, $1H^{C,H}$), 5.36 (d of q, $J_{trans} = 17$ Hz, $J_{geminal} = 1.7$ Hz, $1H^{C,H}$), 5.15 (d of q, $J_{syn} = 10$ Hz, $J_{geminal} = 1.7$ Hz, $1H^{C,H}$), 2.98 (m, $2H^{C,H}$), 2.13 (t, $J = 2.8$ Hz, 1 $H^{C,H}$). Routine ^{13}C NMR spectra were also recorded in $CDCl_3$ at 75 MHz on a Varian Mercury system; ppm 132.1 (C_2), 116.7 (C_1), 81.2 (C_4), 70.8 (C_5), 22.9 (C_3). Proton coupling observed in the 1D spectra was fully supported in the cCOSY, where extensive coupling was observed between all expected vicinal positions, as well as long-range coupling between methylene protons on C_3 to both alkene protons on C_1 and proton H_{11}.

Further purification for the spectroscopic studies was performed with a low-temperature, low-pressure fractionating column and the purity was checked by NMR and infrared spectroscopy. The sample was stored under vacuum at low temperature.

The mid-infrared spectrum of the gas (Figure 1A) was recorded on a Perkin-Elmer model 2000 Fourier transform spectrometer equipped a Ge/CsI beam splitter and DTGS detector. Atmospheric water vapor was removed from the spectrometer housing by purging with dry nitrogen. The spectrum of the gas was obtained by use of a 10-cm cell fitted with CsI windows. The infrared spectrum of the solid (Figure 1B) was obtained by condensing the samples on a CsI substrate held at the temperature of boiling liquid nitrogen, housed in a vacuum cell fitted with a CsI window. The sample was condensed as an amorphous or glassy solid and repeatedly annealed until no further changes were observed in the spectrum.

The mid-infrared spectra (Figure 2A) of the sample dissolved in liquid krypton as a function of temperature were recorded on a Bruker model IFS 66 Fourier transform spectrometer equipped with a Globar source, a Ge/KBr beam splitter, and a TGS detector. A specially designed cryostat cell was used to obtain the spectral data. It consisted of a copper cell with a path length of 4 cm with a wedged silicon window sealed to the cell with indium gaskets. This cell was cooled by boiling liquid nitrogen, and the temperature was monitored with two Pt thermoresistors. The complete cell was connected to a pressure manifold that allows the filling and evacuation of the cell. After the cell had cooled to the designated temperature, a small amount of the compound was condensed into the cell. Next, the pressure manifold and the cell were pressurized with the noble gas, which immediately started to condense in the cell, allowing the compound to dissolve. For all cases 100

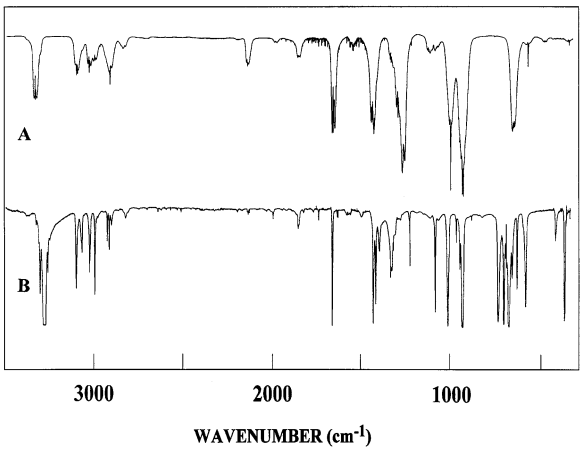

Figure 1. Mid-infrared spectra of 1-penten-4-yne: (A) gas; (B) annealed solid.

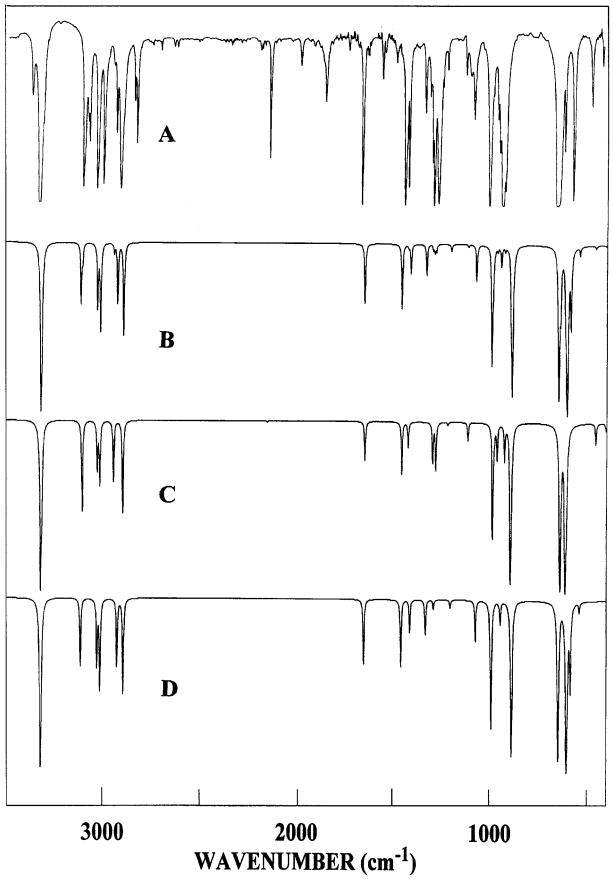

Figure 2. Mid-infrared spectra of 1-penten-4-yne: (A) krypton solution at −125 °C; (B) simulated infrared spectrum of the syn and gauche conformer mixture with $\Delta H = 243$ cm^{-1}; (C) calculated infrared spectrum for the pure gauche conformer; (D) calculated infrared spectrum for the pure syn conformer

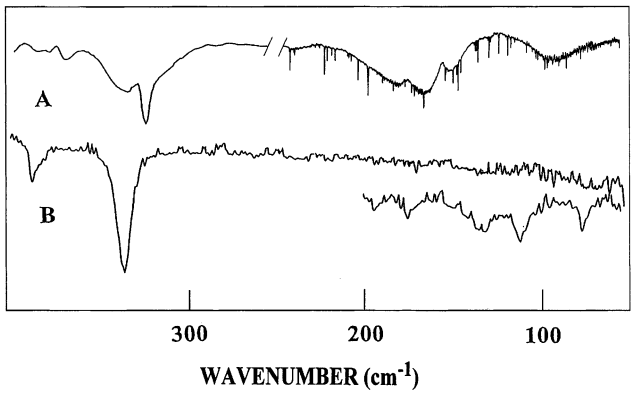

Figure 3. Far-infrared spectra of 1-penten-4-yne: (A) gas with the first part recorded by Perkin-Elmer and the second part recorded by Bomem; (B) annealed solid.

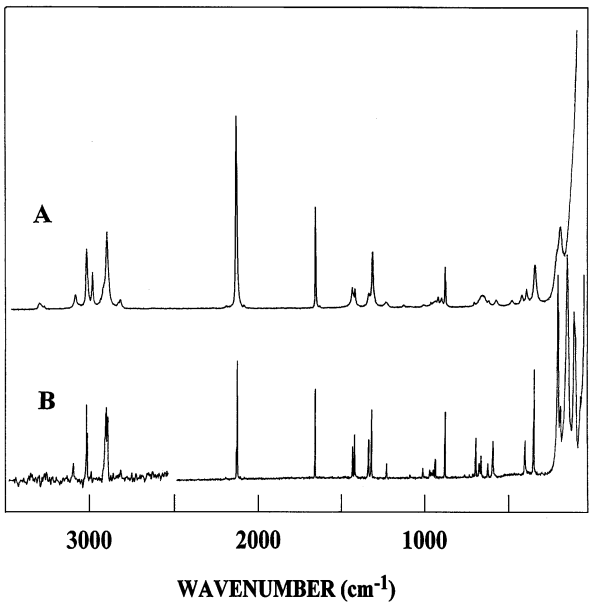

Figure 4. Raman spectra of 1-penten-4-yne: (A) liquid; (B) annealed solid.

interferograms were collected at 1.0 cm^{-1} resolution, averaged, and transformed with a boxcar truncation function.

The far-infrared spectrum of the gas (Figure 3A) was recorded on a Bomem model DA3.002 Fourier transform spectrometer equipped with a vacuum bench, 6.25 and 25 μm Mylar beam splitters, and a liquid helium-cooled Si bolometer. The spectrum was obtained from the sample contained in a 1-m folded path cell equipped with mirrors coated with gold and fitted with polyethylene windows with an effective resolution of 0.1 cm^{-1}. The far-infrared spectra of the amorphous and crystalline solids (Figure 3B) were obtained with the previously described Perkin-Elmer model 2000 equipped with a metal grid beam splitter and a DTGS detector.

The Raman spectra were recorded on a Spex model 1403 spectrophotometer equipped with a Spectra-Physics model 164 argon ion laser operating on the 514.5 nm line. The laser power used was 0.5 W with a spectral band-pass of 3 cm^{-1}. The spectrum of the liquid was recorded with the sample sealed in a Pyrex glass capillary. Depolarization ratio measurements were obtained for the liquid sample by use of a standard Ednalite 35-mm camera polarizer with 38 mm of free aperture affixed to the Spex instrument. Depolarization ratio measurements were checked by measuring depolarization values of the Raman bands of carbon tetrachloride immediately before depolarization measurements were made on the liquid samples. The Raman frequencies are expected to be accurate to ± 2 cm^{-1}, and typical spectra are shown in Figure 4. The wavenumbers for all of the observed bands by the different techniques in the various physical states are listed in Table 1S (Supporting Information).

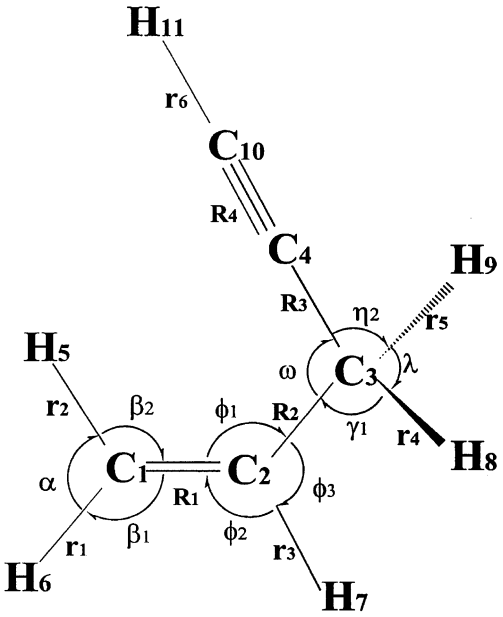

Figure 5. Internal coordinates for 1-penten-4-yne.

Ab Initio Calculations

The electronic structure calculations were performed by the Gaussian-98 program[20] with Gaussian-type basis functions. The energies of 1-penten-4-yne were obtained from restricted Hartree−Fock (RHF) and Møller−Plesset perturbation theory[21] at the second order (MP2) calculation with the 6-31G(d), 6-311G(d,p), and 6-311G(2d,2p) basis sets with full electron correlation along with diffuse functions, and the results are listed in Table 1. The gauche conformer is predicted to be the lower energy rotamer from RHF/6-31G(d), RHF/6-311G(d,p), MP2/6-31+G(d), and MP2/6-311+G(d,p) calculations. However, the syn conformer is predicted to be the more stable form from the calculations with the other basis sets. Density function theory (DFT) calculations were also carried out for the same basis sets by the B3LYP method, and all of these calculations predicted the syn conformer to be the more stable form (Table 1) but with a relatively small energy difference. Therefore, it was necessary to utilize the experimental data to confidently determine the conformational stability.

The optimized values of the structural parameters obtained by several of the ab initio computations are given in Table 2S (Supporting Information) for the syn and the gauche forms. The symbols of the internal coordinate adopted in the present study are also given in this table and shown in Figure 5. The Gaussian 98 program was also employed in calculating the force field in Cartesian coordinates from MP2/6-31G(d) and B3LYP/6-31G-(d) calculations. To obtain a complete assignment of vibrational modes for 1-penten-4-yne, the internal coordinates defined in Table 2S (Supporting Information) and shown in Figure 5 were used to form the symmetry coordinates listed in Table 3S (Supporting Information). The *B*-matrix elements were used to convert the ab initio force field from Cartesian coordinates into the force field in internal coordinates.[22] These force constants were used in a mass-weighted Cartesian coordinate calculation to reproduce the ab initio vibrational frequencies and to

TABLE 1: Calculated Energies and Energy Differences for Syn and Gauche Conformers of 1-Penten-4-yne by ab Initio and Hybrid DFT Methods

method/basis	energy (E_h) for syn conformer	energy difference (cm^{-1}) for gauche conformer[a]
HF/6-31G(d)	−192.739 487	−40
HF/6-311G(d,p)	−192.789 036	−44
MP2(full)/6-31G(d)	−193.391 381	88
MP2(full)/6-31+G(d)	−193.404 677 8	−69
MP2(full)/6-311G(d,p)	−193.574 382	39
MP2(full)/6-311+G(d,p)	−193.579 649	−13
MP2(full)/6-311G(2d,2p)	−193.628 857	212
MP2(full)/6-311+G(2d,2p)	−193.633 672	183
B3LYP/6-31G(d)	−194.042 21	114
B3LYP/6-311G(d,p)	−194.100 571	76
B3LYP/6-311+G(d,p)	−194.103 622	64
B3LYP/6-311G(2d,2p)	−194.108 166	83
B3LYP/6-311+G(2d,2p)	−194.111 487	70

[a] A negative number indicates the gauche conformer is the more stable form.

determine the potential energy distributions (PED), which are given in Table 2 for *syn*- and *gauche*-1-penten-4-yne. The diagonal and off-diagonal elements of the force field in internal coordinates were then modified with scaling factors of 0.88 for the carbon−hydrogen stretches, 0.9 for the heavy atom stretches and carbon−hydrogen bends, and 1.0 for the skeletal bends except for the C≡CC and C≡CH bends, which were scaled with a factor of 1.3. The calculation was repeated to obtain the fixed scaled force field and scaled vibrational frequencies.

The infrared and Raman spectra were simulated with the predicted frequencies, Raman scattering activities, and infrared intensities, which were computed from the MP2/6-31G(d) ab initio calculations. The Raman activity was determined by the previously developed[23,24] analytical gradient method. The activity S_j can be expressed as $S_j = g_j(45\alpha_j^2 + 7\beta_j^2)$, where g_j is the degeneracy of the vibrational mode j, α_j is the derivative of the isotropic polarizability, and β_j is the derivative of the anisotropic polarizability. The Raman scattering cross sections, $\partial\sigma_j/\partial\Omega$, which are proportional to the Raman intensities, can be calculated from the scattering activities and the predicted wavenumbers for each mode.[25,26] To obtain the polarized Raman cross sections, the polarizabilities are incorporated into S_j by $S_j[(1 - \rho_j)/(1 + \rho_j)]$, where ρ_j is the depolarization ratio of the jth normal mode. The Raman scattering cross sections and the calculated wavenumbers were used together with a Lorentzian function to obtain the calculated spectra.

The predicted Raman spectrum of the pure gauche conformer of 1-penten-4-yne is shown in Figure 6C, and that of the pure syn conformer is shown in Figure 6D. The predicted Raman spectrum of the mixture of the two conformers, with an enthalpy difference of 248 cm^{-1}, which was the value obtained from conformational stability studies with the syn conformer as the more stable conformer, is shown in Figure 6B. This result is considered satisfactory when compared to the experimental Raman spectrum (Figure 6A). The major differences are intensities of two lines at 1644 and 1298 cm^{-1} (ν_7 and ν_{11}), which are stronger than those of the predicted spectrum, whereas one line at 562 cm^{-1} (ν_{25}) is stronger in the predicted spectrum than the observed one. In general, the predicted Raman spectrum for the lines in the region 100−1000 cm^{-1} exhibits great similarity with the experimental spectrum and is quite valuable for making the vibrational assignments. Infrared intensities were calculated on the basis of the dipole moment derivatives with respect to the Cartesian coordinates. The derivatives were also taken from the MP2/6-31G(d) ab initio calculation transformed to normal coordinates by $(\partial\mu_u/\partial Q_i) = \Sigma(\partial\mu_u/\partial X_j)L_{ij}$, where Q_i is the ith normal coordinate, X_j is the jth Cartesian displacement coordinate, and L_{ij} is the transformation matrix between the Cartesian displacement coordinates and normal coordinates. The infrared intensities were then calculated by

$$I_i = \frac{N\pi}{3c^2}\left[\left(\frac{\partial\mu_x}{\partial Q_i}\right)^2 + \left(\frac{\partial\mu_y}{\partial Q_i}\right)^2 + \left(\frac{\partial\mu_z}{\partial Q_i}\right)^2\right]$$

Figure 2 spectra C and D are the predicted spectra of pure gauche and syn conformers, respectively. Figure 2B is the predicted spectrum of the mixture utilizing the ΔH value of 248 cm^{-1}, which is in good agreement with the experimental spectrum of the samples dissolved in liquid krypton solution (Figure 2A) at a temperature of −125 °C. However, there are some notable differences. The intensities of the 1285 and 1252 cm^{-1} bands are much stronger than the predicted intensities. Nevertheless, the agreement between the predicted and the observed spectra shows how useful the calculated spectrum can be for making the vibrational assignment for the individual conformers. Such assignments are necessary in order to be able to determine the conformational stability by variable-temperature studies of the infrared bands.

Vibrational Assignment

The syn conformer of 1-penten-4-yne has C_s symmetry and the fundamental vibrations span the irreducible representations 18 A′ + 9 A″. The 18 A′ modes should produce polarized Raman lines and A, B, and A/B hybrid infrared band contours, whereas the nine A″ modes should be depolarized in the Raman spectrum of the liquid and give rise to C-type infrared band contours in the gas spectrum. The gauche conformer has only the trivial C_1 symmetry, and all 27 vibrational modes should yield polarized Raman lines and A, B, C, or A/B/C hybrid-type infrared band contours. The vibrational assignment is based on group frequencies, predicted wavenumbers from ab initio calculations, infrared intensities, Raman activities, and depolarization ratios, as well as the estimated infrared band contours (Figure 7) obtained from the ab initio predicted structural parameters.

Three bands were observed at 1114, 463, and 408 cm^{-1} in the infrared spectrum of 1-penten-4-yne in the krypton solution, with corresponding Raman bands at 1112, 469, and 408 cm^{-1} in the spectrum of the liquid. All three of these bands were absent in the infrared spectrum of the annealed solid. The key to the determination of conformational stability is the band at 463 cm^{-1} (infrared), where there are no other fundamentals observed or predicted between 410 and 540 cm^{-1}. The $C_2C_3C_4$ bend of the gauche conformer is predicted at 457 and 475 cm^{-1} from the MP2/ 6-31G(d) and B3LYP/6-31G(d) calculations,

TABLE 2: Observed and Calculated Wavenumbers (cm^{-1}) for the Syn and Gauche Conformers of 1-Penten-4-yne

		syn conformer									gauche conformer							
vib no.	description	ab initio[a]	fixed scaled[b]	B3LYP	IR int.[c]	Raman act.[d]	gas	Kr	solid	PED[f]	ab initio[a]	fixed scaled[b]	B3LYP	IR int.[c]	Raman act.[d]	gas	Kr	PED[f]
										A′ Species								
ν_1	≡CH stretch	3523	3314	3495	51.4	42.2	3332	3324	3265	$95S_1$	3524	3315	3496	53.6	45.4			$95S_1$
ν_2	=CH_2 antisym stretch	3317	3111	3252	8.0	43.8	3102	3096	3088	$99S_2$	3308	3103	3240	12.0	62.9			$98S_2$
ν_3	=CH_2 sym stretch	3227	3027	3174	7.9	152.8	3031	3024	3015	$73S_3$, $26S_4$	3212	3013	3158	7.4	43.9			$81S_3$, $19S_4$
ν_4	CH stretch	3211	3011	3157	12.1	41.3	2996	2990	2987	$73S_4$, $26S_3$	3226	3026	3172	5.4	112.0			$79S_4$, $17S_3$
ν_5	CH_2 sym stretch	3080	2892	3011	12.8	140.0	2913	2901	2907	$98S_5$	3084	2896	3013	12.3	120.7			$94S_5$
ν_6	C≡C stretch	2174	2154	2244	0.0	54.1	2135	2130	2121	$83S_6$, $12S_{13}$	2172	2152	2241	0.1	65.2			$84S_6$, $12S_{13}$
ν_7	C=C stretch	1737	1648	1736	7.6	3.2	1650	1648	1641	$68S_7$, $14S_9$	1734	1645	1733	4.2	3.2			$67S_7$, $15S_9$
ν_8	CH_2 deformation	1531	1455	1493	7.9	17.7	1429	1423	1416	$94S_8$	1530	1454	1492	5.9	13.1			$95S_8$
ν_9	=CH_2 deformation	1484	1409	1462	3.4	8.5	1406	1406	1400	$79S_9$, $10S_{11}$	1498	1421	1473	2.6	7.8			$75S_9$, $10S_{11}$
ν_{10}	CH_2 wag	1397	1328	1371	3.7	14.2	1326	1322	1318	$66S_{10}$, $12S_{14}$	1363	1294	1346	4.3	14.1	1286	1285	$59S_{10}$, $15S_{11}$, $11S_7$
ν_{11}	CH bend	1353	1286	1336	0.9	9.9	1301	1299	1302	$58S_{11}$, $15S_{12}$, $13S_7$	1345	1278	1327	5.3	6.7	1254	1252	$50S_{11}$, $27S_{10}$
ν_{12}	=CH_2 wag	1121	1070	1101	4.4	1.0	1071	1070	1065	$37S_{12}$, $18S_{10}$, $11S_{11}$	1162	1112	1139	1.9	1.1	1115	1114	$22S_{12}$, $20S_{14}$, $17S_{20}$, $14S_{22}$, $11S_{11}$
ν_{13}	C_3C_4 stretch	992	943	972	2.3	0.7	930	924	926	$33S_{13}$, $31S_{12}$, $20S_{14}$	1010	962	988	3.7	1.7	940	939	$48S_{13}$, $19S_{14}$
ν_{14}	C_2C_3 stretch	898	866	873	0.2	6.3	847	862	862	$40S_{14}$, $26S_{13}$, $10S_{16}$	959	924	947	3.9	5.2	908	908	$16S_{14}$, $40S_{22}$, $10S_{16}$
ν_{15}	C≡CH in-plane bend	537	648	611	39.2	0.3	636	645	681	$62S_{15}$	555	639	618	48.7	0.6			$42S_{15}$, $13S_{25}$
ν_{16}	$C_2C_3C_4$ bend	623	586	628	11.1	1.3	603	604	606	$25S_{16}$, $41S_{15}$, $17S_{17}$	449	457	475	2.2	2.0	461	463	$31S_{16}$, $32S_{26}$, $12S_{25}$
ν_{17}	C=CC bend	371	381	382	0.3	2.6	376		387	$53S_{17}$, $34S_{18}$	409	405	409	0.8	3.0	406	408	$75S_{17}$
ν_{18}	C≡CC in-plane bend	155	166	167	0.1	7.4	162		186	$53S_{18}$, $42S_{16}$	293	328	341	0.2	9.3			$89S_{18}$
										A″ Species								
ν_{19}	CH_2 antisym stretch	3119	2926	3030	8.0	89.6	2927	2926	2916	$100S_{19}$	3137	2943	3064	7.0	68.0			$95S_{19}$
ν_{20}	CH2 twist	1263	1200	1247	0.8	6.0	1213	1209	1208	$97S_{20}$	1278	1216	1257	0.3	9.1		1233	$75S_{20}$
ν_{21}	=CH_2 twist	1043	990	1034	21.7	0.5	992	990	994	$57S_{21}$, $36S_{25}$	1037	984	1033	17.7	0.4	975	974	$59S_{21}$, $35S_{25}$
ν_{22}	CH_2 rock	992	951	973	0.1	3.7	952	950	947	$73S_{22}$, $14S_{21}$	924	884	905	0.8	2.9			$24S_{22}$, $37S_{12}$, $12S_{13}$
ν_{23}	=CH_2 rock	934	886	947	35.9	0.0	920	919	912	$98S_{23}$	941	892	935	40.3	0.1	926	921	$95S_{23}$
ν_{24}	C≡CH out-of-plane bend	525	605	567	61.6	0.6	632	632	651	$91S_{24}$	542	613	598	52.2	0.0			$49S_{24}$, $37S_{15}$
ν_{25}	CH bend	577	540	601	1.0	15.0	557	557	557	$47S_{25}$, $25S_{21}$, $19S_{22}$	654	607	644	9.4	9.3			$14S_{25}$, $48S_{24}$, $18S_{15}$
ν_{26}	C≡CC out-of-plane bend	267	303	342	0.3	8.5	322		334	$92S_{26}$	172	185	188	0.1	12.8	179		$53S_{26}$, $35S_{16}$
ν_{27}	asym torsion	138	139	150	0.1	2.2	138		165	$92S_{27}$	91	91	90	0.0	8.8	96		$76S_{27}$

[a] Calculated at the MP2/6-31G* level. [b] Scaled ab initio calculations with factors of 0.88 were used for the C−H stretches, 0.9 for the heavy atom stretches and CH bends, 1.3 for C≡C in-plane and out-of-plane bends, and 1.0 for all other modes with the MP2/6-31G* calculations. [c] Calculated infrared intensities in kilometers per mole with the MP2/6-31G* basis set. [d] Calculated Raman activities in angstroms^4 per atomic mass unit with the MP2/6-31G* basis set. [e] Observed solid frequencies are from the infrared spectrum. [f] Potential energy distributions, calculated for the MP2/6-31G* basis set; contributions less than 10% are omitted.

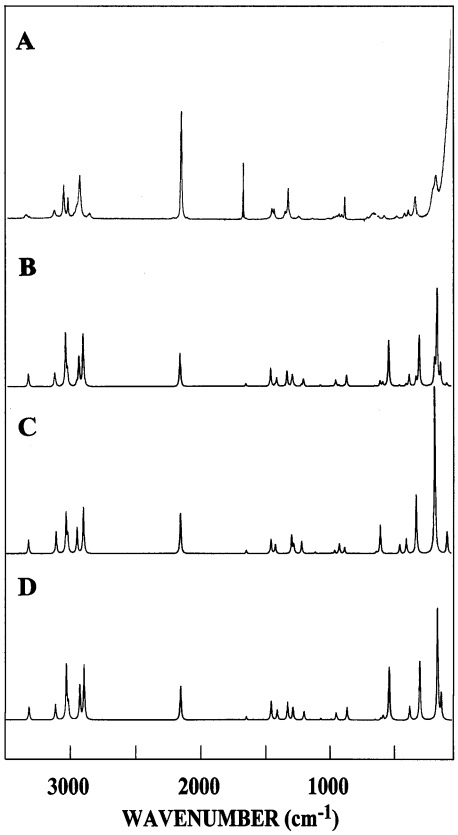

Figure 6. Raman spectra of 1-penten-4-yne: (A) liquid; (B) simulated Raman spectrum of the syn and gauche conformer mixture with $\Delta H = 243$ cm^{-1}; (C) calculated Raman spectrumfor the pure gauche conformer; (D) calculated Raman spectrum for the pure syn conformer.

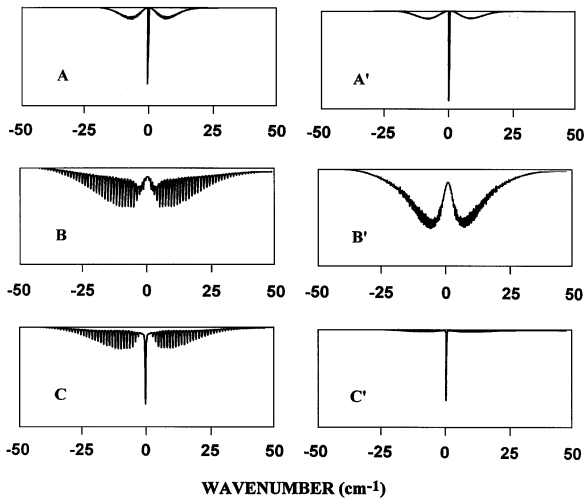

Figure 7. Predicted pure A-, B- and C-type infrared band contours for the gauche (unprimed) and syn (primed) conformers of 1-penten-4-yne.

respectively, with the closest predicted syn fundamentals at 380 and 540 cm^{-1}. Thus, the 463 cm^{-1} band can be confidently assigned as a fundamental of the gauche conformer. Therefore, all bands that disappear from the infrared and Raman spectra of the gas or liquid can be assigned to the gauche conformer, and it is reasonable to assign all bands in the spectrum of the well-annealed solid to the syn conformer.

The assignment of the CH stretches and CH_2 bends is straightforward based on "group frequencies", infrared band contours, relative intensities, and the predictions from the ab

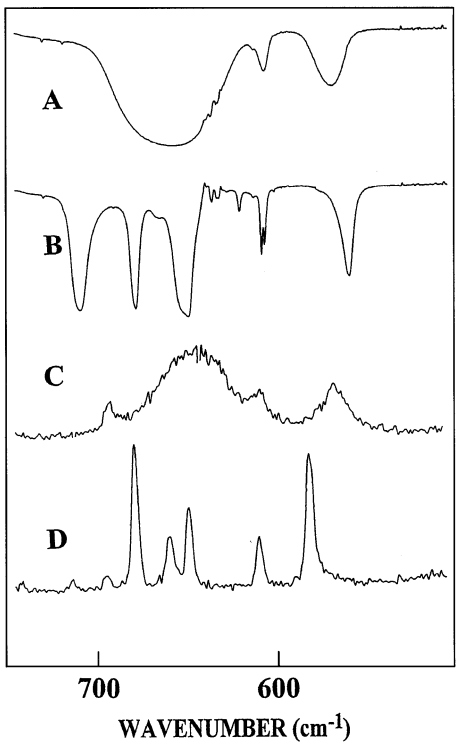

Figure 8. Vibrational spectra of 1-penten-4-yne (500−750 cm^{-1}): (A) infrared spectrum of amorphous solid; (B) infrared spectrum of annealed solid; (C) Raman spectrum of liquid; (D) Raman spectrum of annealed solid.

initio predictions. However, the challenge is the assignment of the heavy atom motions, particularly the low-frequency bending modes of the C−C≡C−H group. The MP2/6-31G(d) ab initio predicted frequencies for hydrocarbon are usually too high by about 5% but this is not the case for C≡C−H group, where the bending modes, particularly the out-of-plane motions, are predicted too low by more than 15%. Thus the scaling of the force constants for these bends by 1.3 results in predicted frequencies for these modes, which makes their assignments reasonably easy.

The C≡CC out-of-plane bend is assigned to the peak at 322 cm^{-1} in the infrared spectrum of the gas, where the predicted value is only 303 cm^{-1}. However, the prediction from the B3LYP/6-31G(d) calculation of this mode is 342 cm^{-1}, so the observed band is about halfway between the predicted values. The most difficult part of the assignment is for the ≡C−H bends. The in-plane and out-of-plane bends are assigned to the bands at 645 and 632 cm^{-1}, respectively, in the infrared spectrum of the krypton solution. Upon comparison of this spectrum to the infrared spectrum of the solid, it is clear that these two bands split into four peaks at 712, 681, 651, and 635 cm^{-1}. The remaining fundamental mode of interest is the asymmetric torsion, which is observed as a broad weak absorption centered near 96 cm^{-1} (Figure 3) in the spectrum of the gas. However, there are a series of *Q*-branches beginning at 138 cm^{-1}, which must be due to the syn conformer. There is a maximum at 96.2 cm^{-1}, which is assigned as the asymmetric torsional fundamental of the gauche conformer. These assignments are in reasonable agreement with the ab initio predicted frequencies, although the assignment for the gauche conformer torsional mode is 6 cm^{-1} higher than the predicted value.

Upon comparison of the infrared spectrum of the polycrystalline solid with that of amorphous solid, many bands are observed to be split in the solid state (Figure 8). For example,

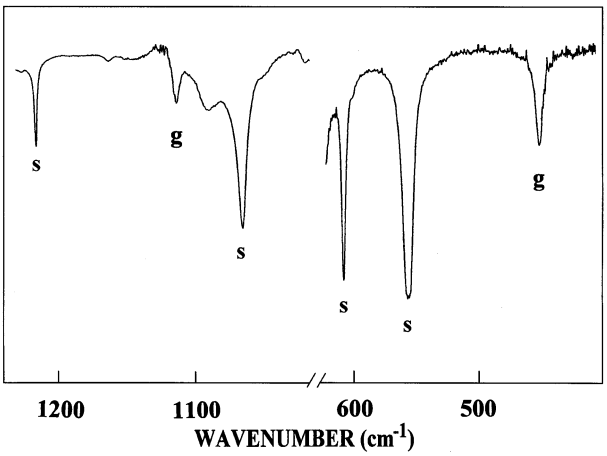

Figure 9. Mid-infrared spectrum of 1-penten-4-yne dissolved in liquid krypton at −125 °C (1020−1220 and 420−610 cm^{-1}).

the fundamental ν_{16} is split into a pair of peaks at 609/606 cm^{-1}. Similar splittings are also observed for the ν_{15} , ν_{17}, and ν_{24} fundamentals. Therefore, there must be at least two molecules per primitive cell in the crystal.

Conformational Stability

To obtain the value of the enthalpy difference between the two conformers similar to the values expected for the gas, variable-temperature studies in liquefied krypton were carried out. Only small frequency shifts are anticipated when passing from the gas phase to the krypton solution,[27−31] which is exactly what was found. Also, the areas of the conformer peaks are more accurately determined than those from the spectrum of the gas and there is excellent control of the temperature.

Only a limited number of gauche fundamentals can be used to determine the enthalpy difference since most of those identified are close to syn fundamentals. The 463 cm^{-1} band is an obvious choice (Figure 9), and the 1114 cm^{-1} band is reasonably free of interference. There are several syn bands to choose from, so bands well separated from the gauche bands with similar intensity were chosen, i.e., 557, 1070, and 1209 cm^{-1} bands. From these bands, five conformer pairs were used to determine the enthalpy difference between the syn and gauche conformers. The spectral changes of the solution were recorded as a function of temperature from −105 to −150 °C. The conformer pair 1209/463 cm^{-1} (Figure 10), where the first wavenumber is for the syn conformer, shows the increased intensity for the syn conformer as the temperature decreases, which is consistent with the prediction from the MP2/6-311+G-(2d,2p) ab initio calculation that the syn form is the more stable conformer. The ΔH value was determined from a van't Hoff plot of $-\ln K$ versus $1/T$, where $\Delta H/R$ is the slope of the line and the intensity ratio I_{syn}/I_{gauche} is substituted for K. It is assumed that ΔH is not a function of temperature over the relatively small temperature range. The determined ΔH values ranged from a high value of 294 ± 9 cm^{-1} to a low value of 189 ± 10 cm^{-1}, with the syn conformer as the more stable form (Table 3). This enthalpy difference should be close to the value in the vapor state[27−31] since the two conformers have similar molecular volumes and their dipole moments probably differ by less than 10%. The average of the five values is 248 ± 11 cm^{-1} (2.96 ± 0.13 kJ/mol), where the uncertainty is statistical, which does not take into account factors such as the presence of overtone or combination bands in near coincidence with the measured fundamentals. Therefore, a more realistic value for the uncertainty should be at least 10%, which results in a value of 248 ± 25 cm^{-1} (2.96 ± 0.30 kJ/mol) for the enthalpy difference.

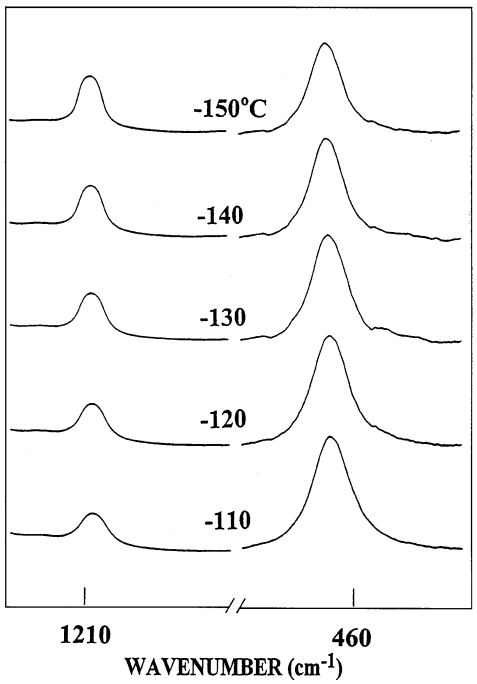

Figure 10. Temperature-dependent (−150 to −110 °C) infrared spectrum of 1-penten-4-yne in liquid krypton for the syn (1207 cm^{-1}) and the gauche (460 cm^{-1}) conformer bands.

With the ΔH value of 248 ± 25 cm^{-1}, the abundance of the gauche conformer is 38% ± 2% at room temperature, so it should be possible to obtain the structural parameters and relative stability from the microwave spectra of both conformers. It would be interesting to compare the experimental values to those obtained from ab initio calculations.

Discussion

The experimental data clearly show the syn conformer to be the more stable form with an enthalpy difference of 248 ± 25 cm^{-1}. It should be noted that the ab initio calculations do not give the correct prediction for the conformational stability with all of the basis sets. For example, both RHF/6-31G(d) and MP2/6-311+(d,p) calculations predicted the gauche conformer to be the more stable conformer with enthalpy differences of 40 and 13 cm^{-1}, respectively. However, the largest basis set utilized, i.e., MP2/6-311+G(2d,2p), gives the correct prediction with an energy difference of 183 cm^{-1}, which is in excellent agreement with the experimental results. Similar problems have been reported in some previous studies[32−35] where the ab initio calculations with smaller basis sets give incorrect conformational predictions. Therefore, to obtain the correct conformational stability prediction from ab initio calculations, relatively large basis sets are necessary and the results should be confirmed by experimental data when possible.

The theoretically predicted energy difference ranges from the lowest value of −69 cm^{-1}, with the gauche conformer as the more stable form [MP2/6-31+G(d)], to the highest value of 212 cm^{-1}, with the syn conformer as the more stable form (Table 1). These calculations also showed that the basis sets with diffusion functions give smaller energy differences between the gauche and syn forms than those without diffusion functions. The DFT calculations by B3LYP method are consistent with those of the MP2 calculations but with a smaller value of this

TABLE 3: Temperature and Intensity Ratios from Conformational Study of 1-Penten-4-yne in Liquid Krypton Solution[a]

T (°C)	1000/T (K)	I_{557}/I_{463}[b]	I_{1070}/I_{463}[c]	I_{1209}/I_{460}[d]	I_{557}/I_{1114}[e]	I_{1070}/I_{1114}[f]
−105	5.952	1.437	1.347		31.26	4.060
−110	6.129	1.496	1.443	0.134	31.87	4.403
−115	6.323	1.600	1.495	0.158		
−120	6.530	1.638	1.790	0.170		5.221
−125	6.750	1.720	1.981	0.195	33.25	
−130	6.986	1.752	2.120	0.209		6.338
−135	7.239	1.796	2.195	0.224	34.92	7.759
−140	7.510	1.885	2.453	0.252	49.35	8.342
−145	7.803	2.016	2.851		49.84	8.870
−150	8.120	2.022	2.998	0.327	63.80	9.809

[a] Average value of ΔH is 248 ± 11 cm^{-1} (2.96 ± 0.13 kJ mol^{-1}) with the syn conformer the more stable form. [b] ΔH^a = 189 ± 10 cm^{-1}. [c] ΔH^a = 263 ± 14 cm^{-1}. [d] ΔH^a = 294 ± 9 cm^{-1}. [e] ΔH^a = 215 ± 44 cm^{-1}. [f] ΔH^a = 294 ± 16 cm^{-1}.

energy difference. This tendency is much more obvious for 3-fluoropropene,[2] where two diffuse functions were utilized. Therefore, the inclusion of the diffusion functions tends to give a smaller energy difference between stable conformers for unsaturated molecules such as 1-penten-4-yne.

The difference between predicted and observed frequencies is 11 cm^{-1} for the A′ block and 13 cm^{-1} for the A″ block for the syn conformer, which represents an average error of 0.9%. The average error for the observed fundamentals for the gauche conformers is 12 cm^{-1}. Therefore, the predictions from the MP2/6-31G(d) calculations with three scaling factors for the force constants provide excellent predictions for the fundamental frequencies of these types of hydrocarbons.

The potential energy distributions (PED) are relatively pure for the syn conformer (Table 2), with only five modes significantly mixed. The =CH_2 wag (ν_{12}) has only 37% contribution from this motion. The remaining contributors are the C_3C_4 stretch (ν_{13}), C_2C_3 stretch (ν_{14}), $C_2C_3C_4$ bend (ν_{16}), and CH bend (ν_{25}). The mixing is much more extensive for the gauche conformer (Table 2), where seven modes have contributions of less than 50% as the major contributor to the fundamental. For example, the ν_{25} and ν_{12} fundamentals have only 14% and 22% contribution from the indicated vibrational descriptions. Thus, the descriptions given for the normal modes of the gauche conformer are more for bookkeeping than to give an accurate description of atomic motions for several of the modes in the "fingerprint" spectral region.

The potential function governing the conformational interconversion was obtained from the experimental data as well as prediction from the ab initio calculations. The torsional potential is represented by a Fourier cosine series in the internal rotation angle ϕ:

$$V(\phi) = \sum_{i=1}^{6}\left(\frac{V_i}{2}\right)(1 - \cos i\phi)$$

where ϕ and i are the torsional angle and foldness of the barrier, respectively. The internal rotation constant $F(\phi)$, which is used to calculated the potential function, also varies as a function of the internal rotation angle, and this is approximated by another Fourier series:

$$F(\phi) = F_0 + \sum_{i=1}^{5} F_i \cos i\phi$$

The relaxation of the structural parameters, $B(\phi)$, during the internal rotation can be incorporated into the above equation by assuming them to be small periodic functions of the torsional angle of the general type $B(\phi) = a + b\cos\phi + c\sin\phi$.

TABLE 4: Potential Barriers (cm^{-1}) and Coefficients (cm^{-1}) of 1-penten-4-yne Determined from Far Infrared Spectra and from ab Initio Calculations

coefficients	experimental[a]	MP2/6-31G(d)
V_1	166 ± 28	−5
V_2	211 ± 6	170
V_3	710 ± 2	800
V_4	−15 ± 4	−25
V_5		−14
V_6		−47
ΔH	248 ± 36	87
ΔE	269	90
potential barriers		
syn → gauche	909	908
gauche → gauche	607	691
gauche → syn	641	819
dihedral angle (deg)	122.6[b]	123.4

[a] Calculated from F_0 = 2.012 998, F_1 = 0.528 025, F_2 = 0.282 508, F_3 = 0.070 860, F_4 = 0.029 068, F_5 = 0.008 078, and F_6 = 0.003 170 cm^{-1}. [b] From MP2/6-311+G(d,p) calculation.

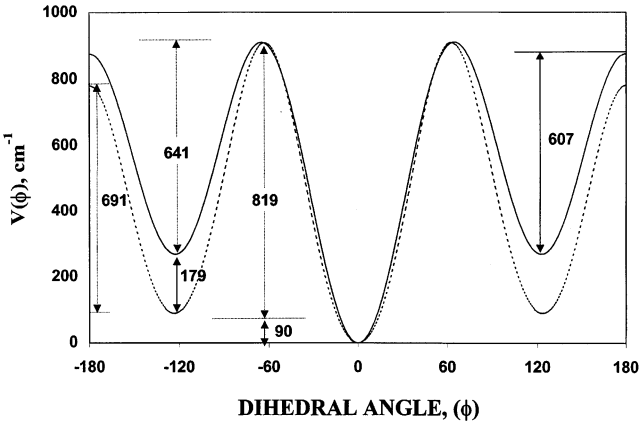

Figure 11. Potential function governing the internal rotation of 1-penten-4-yne as determined from ab initio calculations [dotted line, MP2/6-31(d)] and from spectral data (solid line).

The 1←0 torsional transitions for the syn and gauche conformers were assigned to the infrared peaks at 138 and 96 cm^{-1}, respectively. The additional transitions for the syn rotamer with successive excited states were assigned to bands at 129, 122, and 113 cm^{-1} in the infrared spectrum of gas. By utilizing the experimental determined enthalpy and the torsional angle from the ab initio calculations, we obtained the experimental fitted potential function for 1-penten-4-yne (Figure 11). The syn to gauche, gauche to syn, and gauche to gauche barriers are 909, 641, and 607 cm^{-1}, respectively. For the purpose of comparison, the predicted potential function was also calculated with theMP2/6-31G(d) basis set (Figure 11). The V_2 to V_4 potential terms are very close to the experimental determined data, whereas the V_1 term is significantly different (Table 4).

TABLE 5: Comparison of Some Structural Parameters of 3-Fluoropropene,[a] Allyl Cyanide, and 1-Penten-4-yne[b]

	3-fluoropropene				allyl cyanide				1-penten-4-yne[c]	
	syn		gauche		syn		gauche			
parameter	ab initio[c]	r_0[d]	ab initio[c]	r_0[d]	ab initio[c]	r_0[d]	ab initio[c]	r_0[d]	syn	gauche
r(C═C)	1.338	1.337	1.339	1.339	1.338	1.338	1.338	1.338	1.339	1.339
$r(C_2-C_3)$	1.496	1.493	1.492	1.490	1.510	1.510	1.508	1.507	1.511	1.508
$r(C_3-C_4/F)$	1.389	1.389	1.399	1.399	1.462	1.462	1.466	1.466	1.461	1.465
$r(C_1-H_5)$	1.084	1.084	1.086	1.086	1.086	1.086	1.086	1.086	1.085	1.085
$r(C_1-H_6)$	1.084	1.084	1.084	1.084	1.084	1.084	1.084	1.084	1.085	1.086
$r(C_2-H_7)$	1.089	1.089	1.088	1.087	1.088	1.088	1.088	1.088	1.089	1.088
$r(C_3-H_8)$	1.095	1.095	1.094	1.094	1.096	1.096	1.096	1.096	1.097	1.097
$r(C_3-H_9)$	1.095	1.095	1.093	1.093	1.096	1.096	1.094	1.094	1.097	1.095
$\angle C_1C_2C_3$	124.5	124.4	122.8	122.8	125.2	125.2	123.1	123.0	125.4	123.6
$\angle C_2C_3C_4(F)$	111.6	111.6	109.9	110.0	113.3	113.2	111.6	111.4	114.3	111.8
$\angle C_2C_1H_5$	121.1	121.1	121.1	121.1	121.7	121.7	121.4	121.4	120.6	121.0
$\angle C_2C_1H_6$	120.7	120.7	121.5	121.5	120.5	120.5	121.0	121.0	121.2	121.2
$\angle C_1C_2H_7$	120.6	120.3	120.7	120.4	120.1	120.1	120.4	120.5	119.7	120.2
$\tau[C_1C_2C_3C_4(F)]$	0.0	0.0	122.9	125.6	0.0	0.0	121.7	125.8	0.0	122.6

[a] Reference 2. [b] Reference 7. [c] Results from MP2/6-311+G(d,p) calculations. [d] Microwave adjusted data by use of MP2/6-311+G(d,p) result.

TABLE 6: Comparison of Rotational Constants[a] Obtained from Modified ab Initio Calculation Results with Experimentally Determined Data from Microwave Spectra for Allyl Fluoride[b] and Allyl Cyanide[c]

		syn			gauche		
molecule	rotational constants	obs	calc	D	obs	calc	D
CH_2═$CHCH_2F$	A	17 236.63	17 237.83	1.20	27 720.34	27 722.30	1.96
	B	6002.91	6003.11	0.20	4263.62	4263.64	0.03
	C	4579.82	4580.05	0.23	4131.98	4132.22	0.24
CH_2═$^{13}CHCH_2F$	A	17 042.88	17 042.38	0.50	27423.89	27 422.02	1.87
	B	5952.98	5952.84	0.14	4241.00	4241.07	0.07
	C	4537.04	4537.00	0.04	4111.29	4111.06	0.23
$^{13}CH_2$═$CHCH_2F$	A	17 060.59	17 060.55	0.04			
	$B/(B+C)$	5844.26	5843.95	0.31	8156.22	8156.16	0.06
	C	4474.83	4474.72	0.11			
CH_2═$CH^{13}CH_2F$	A	16 964.23	16 963.26	0.97			
	$B/(B+C)$	5973.92	5973.97	0.05	8367.54	8367.55	0.01
	C	4543.57	4543.60	0.03			
CH_2═$CHCH_2CN$	A	11 323.01	11 321.89	1.12	19 707.99	19 707.19	0.80
	B	3739.20	3738.00	1.20	2619.74	2619.37	0.37
	C	2858.52	2859.68	1.16	2497.43	2497.88	0.45

[a] Rotational constants are given in megahertz. [b] Reference 39. [c] Reference 35.

This result is reasonable because ΔE from the MP2/6-31G(d) calculations is only 88 cm^{-1}, which is much smaller than the experimental result of 248 cm^{-1} for the enthalpy difference.

The structural parameters and the force constants for the syn and gauche conformers are essentially the same with few exceptions (Table 2S, Supporting Information). The predicted bond distances are nearly the same for the two conformers with maximum difference of 0.004 Å for the C_3C_4 bond, with the gauche conformer having a larger value. The bond distances of C_2C_3 and C_3H_9 for the gauche conformer are respectively 0.003 and 0.002 Å longer than those of the syn conformer. The angles of $C_2C_3C_4$ and $C_1C_2C_3$ for the syn form are predicted to be respectively 2.5° and 1.8° larger than those of the gauche conformer. The largest difference of the force constants comes from the $C_2C_3C_4$ bend (ω), which increases 25.9% in the syn conformer compared with the gauche conformer. Such a large difference brings a significant change to the corresponding $C_2C_3C_4$ bending modes, which are found at 604 and 463 cm^{-1} in the infrared spectra of the krypton solution for the syn and gauche conformers, respectively. The gauche band shifts about 140 cm^{-1} to the low-frequency region. The force constants for the C═CC bend (ν_{17}) are also quite different between the syn and gauche conformers, with the one for the syn conformer about 17.8% higher than that for the gauche conformer. Therefore, the skeletal bending modes have the largest differences in frequencies between the two conformers. Additionally, the force constants of $H_8C_3H_9$ (λ) and $C_2C_3H_8$ (ϕ_3) changed by 10% and 7.6%, respectively, between two conformers.

It is interesting to compare the conformational and structural results between 1-penten-4-yne and 1-hexen-4-yne,[36] where the only difference is the replacement of H on the carbon with the triple bond with a methyl group in the former molecule. The syn conformer is the more stable rotamer in both fluid and solid states for both molecules. The predicted energy differences are 88 and 95 cm^{-1}, respectively, for 1-penten-4-yne and 1-hexen-4-yne from the MP2/6-31G(d) calculations. According to the ab initio MP2/6-31G(d) calculation, the C≡C distance is 0.002 Å longer and $\angle C_1C_2C_3$ is 0.01° larger in 1-penten-4-yne than in 1-hexen-4-yne. The corresponding torsional angles $\tau(C_1C_2C_3C_4)$ are 125.1° and 123.3°, respectively, with 1-penten-4-yne having a slightly larger value. The experimental values for the enthalpy difference are 248 ± 25 and 233 ± 23 cm^{-1}, respectively, for 1-penten-4-yne and 1-hexen-4-yne. Therefore, the substitution of a methyl group for the hydrogen atom on the triple bond does not have any significant effect on conformational behavior or structural parameters of these two molecules.

Since allyl cyanide, CH_2═$CHCH_2CN$, is isoelectronic with

1-penten-4-yne, we have determined the structural parameters for the cyanide for comparison with the acetylenic molecule (Table 5). We have found[2] that one can obtain good structural parameters by adjusting the structural parameters obtained from the ab initio calculations to fit rotational constants (computer program A&M, ab initio and microwave, developed in our laboratory) obtained from the microwave experimental data. To reduce the number of independent variables, the structural parameters are separated into sets according to their types. Bond lengths in the same set keep their relative ratio, and bond angles in another set keep their differences in degrees. This assumption is based on the fact that the errors from ab initio calculations are systematic.

The microwave spectra of the two conformers of allyl cyanide have been reported,[37] so there are six rotational constants for the determination of the six heavy-atom parameters, excluding the C≡N distance. The value for this bond length has been determined for a number of XCN molecules[38,39] and the triple bond does not vary significantly with X substitution. Since the MP2/6-311+G(d,p) calculations predict r_0 C−H distances for hydrocarbons within 0.003 Å of the determined values obtained from "isolated" C−H stretching frequencies,[40] we have kept the carbon−hydrogen parameters the same as predicted from the MP2/6-311+G(d,p) calculations. For the syn conformer of the cyanide, after adjustment of the parameters, the fit of the calculated *A* rotational constant is too small by 1.1 MHz, whereas the *B* and *C* constants are too larger by 1.2 and 1.16 MHz, respectively, compared to the experimentally determined values (Table 6). For the gauche conformer, the fit of the predicted rotational constants from the adjusted parameters to the experimental ones is even better with differences of only 0.8, 0.37, and 0.45 MHz, respectively (Table 6). Therefore, only very minor adjustments were needed for the predicted ab initio MP2/6-311+G(d,p) parameters of the two conformers to fit all six rotational constants (Table 5).

To demonstrate this procedure of utilizing the ab initio MP2/6-311+G(d,p) values for the C−H distances, with the fit of the heavy-atom isotopomer's rotational constants, we also carried out a similar calculation for 3-fluoropropene. Four sets of rotational constants that were reported from the microwave study[41] were used (Table 6). Again, with only minor adjustments of the heavy-atom parameters (Table 5), there is an excellent fit to all 20 experimentally determined rotational constants. There are only three constants where the difference is greater than 1 MHz. As can be seen from the structural data listed in Table 5, the adjustment of the parameter values for the two conformers is quite small. Therefore, it is believed that the predicted structural parameters for 1-penten-4-yne should have uncertainties not greater than 0.005 Å for the heavy atoms, 0.003 Å for CH bond distances, and 0.5° for the angles.

Acknowledgment. J.R.D. acknowledges the University of Missouri−Kansas City for a Faculty Research grant for partial financial support of this research.

Supporting Information Available: Table 1S, listing the complete vibrational assignment for observed bands for 1-penten-4-yne; Table 2S, listing structural parameters, rotational constants, dipole moments, and energies for 1-penten-4-yne; Table 3S, listing symmetry coordinates; Table 4S, listing the comparison of the structural parameters of 3-fluoropropene and allyl cyanide; and Tables 5S and 6S, listing harmonic force constants from ab initio calculations for the syn and gauche conformers for 1-penten-4-yne. This material is available free of charge via the Internet at http://pubs.acs.org.

References and Notes

(1) Durig. J. R.; Zhen, M.; Heusel, H. L.; Joseph, P. J.; Groner, P.; Little, T. S. *J. Phys. Chem. A* **1985**, *89*, 2877.

(2) van der Veken, B. J.; Herrebout, W. A.; Durig, D. T.; Zhao, W.; Durig, J. R. *J. Phys. Chem. A* **1999**, *103*, 1976.

(3) Durig, J. R.; Durig, D. T.; van der Veken, B, J.; Herrebout, W. A. *J. Phys. Chem. A* **1999**, *103*, 6142.

(4) Durig, J. R.; Tang, Q.; Little, T. S. *J. Mol. Struct.* **1992**, *269*, 257.

(5) Durig, D. T.; Yu, Z. *J. Mol. Struct.* **2000**, *550/551*, 481.

(6) Durig, J. R.; Tang, Q.; Little, T. S. *J. Raman Spectrosc.* **1992**, *23*, 653.

(7) Durig, J. R.; Guirgis, G. A.; Drew, A. S. *J. Raman Spectrosc.* **1994**, *25*, 907.

(8) Bell, S.; Drew, B. R.; Guirgis, G. A.; Durig, J. R. *J. Mol. Struct.* **2000**, *553*, 199.

(9) Guirgis, G. A.; Nashed, Y. E.; Gounev, T. K.; Durig, J. R. *Struct. Chem.* **1998**, *9*, 265.

(10) Botskar, I.; Rudolph, H. D.; Roussy, G. *J. Mol. Spectrosc.* **1974**, *53*, 15.

(11) Botskar, I.; Rudolph, H. D.; Roussy, G. *J. Mol. Spectrosc.* **1974**, *52*, 457.

(12) Silvi, B.; Perchard, J. P. *Spectrochim. Acta* **1976**, *32A*, 23.

(13) Durig, J. R.; Sullivan, J. F.; Whang, C. M. *Spectrochim. Acta* **1985**, *41A*, 129.

(14) Murty, A. N.; Curl, R. F., Jr. *J. Chem. Phys.* **1967**, *46*, 4176.

(15) Silvi, B.; Perchard, J. P. *Spectrochim. Acta* **1976**, *32A*, 11.

(16) Galabov, B.; Kenny, J. P.; Schaefer, H. F., III; Durig, J. R. *J. Phys. Chem. A* **2002**, *106*, 3625.

(17) Inamoto, N.; Masuda, S. *Chem. Lett.* **1982**, 1003.

(18) Davini, E.; Giongo, M.; Riocci, M. *Org. Prep. Proced. Int.* **1995**, *27*, 586.

(19) Pritchard, A. *Ann. Phys. (Paris)* **1966**, *1*, 127.

(20) Frisch, M. J.; Trucks, G. W.; Schlegel, H. B.; Scuseria, G. E.; Robb, M. A.; Cheeseman, J. R.; Zakrzewski, V. G.; Montgomery, J. A., Jr.; Stratmann, R. E.; Burant, J. C.; Dapprich, S.; Millam, J. M.; Daniels, A. D.; Kudin, K. N.; Strain, M. C.; Farkas, O.; Tomasi, J.; Barone, V.; Cossi, M.; Cammi, R.; Mennucci, B.; Pomelli, C.; Adamo, C.; Clifford, S.; Ochterski, J.; Petersson, G. A.; Ayala, P. Y.; Cui, Q.; Morokuma, K.; Malick, D. K.; Rabuck, A. D.; Raghavachari, K.; Foresman, J. B.; Cioslowski, J.; Ortiz, J. V.; Stefanov, B. B.; Liu, G.; Liashenko, A.; Piskorz, P.; Komaromi, I.; Gomperts, R.; Martin, R. L.; Fox, D. J.; Keith, T.; Al-Laham, M. A.; Peng, C. Y.; Nanayakkara, A.; Gonzalez, C.; Challacombe, M.; Gill, P. M. W.; Johnson, B. G.; Chen, W.; Wong, M. W.; Andres, J. L.; Head-Gordon, M.; Replogle, E. S.; Pople, J. A. *Gaussian 98*, revision A.7; Gaussian, Inc.: Pittsburgh, PA, 1998.

(21) Moller, C.; Plesset, M. S. *Phys. Rev.* **1934**, *46*, 618.

(22) Guirgis, G. A.; Zhu, X.; Yu, Z.; Durig, J. R. *J. Phys. Chem. A* **2000**, *104*, 4383.

(23) Frisch, J. M.; Yamagushi, Y.; Gaw, J. F.; Schaefer, H. F., III; Binkley, J. S. *J. Chem. Phys.* **1986**, *84*, 531.

(24) Amos, R. D. *Phys. Lett.* **1986**, *124*, 374.

(25) Polavarapu, P. L.*J. Phys. Chem.* **1990**, *94*, 8106.

(26) Chantry, W. G. In *The Raman Effect*; Anderson, A., Ed.; Marcel Dekker Inc.: New York, 1971; Vol. 1, Chapt. 2.

(27) Bulanin, M. O. *J. Mol. Struct.* **1973**, *19*, 59.

(28) van der Veken, B, J.; DeMunck, F. R. *J. Chem. Phys.* **1992**, *97*, 3060.

(29) Bulanin, M. O. *J. Mol. Struct.* **1995**, *347*, 73.

(30) Herrebout, W. A.; van der Veken, B. J.; Wang, A.; Durig, J. R. *J. Phys. Chem.* **1995**, *99*, 578.

(31) Herrebout, W. A.; van der Veken, B. J. *J. Phys. Chem.* **1996**, *100*, 9671.

(32) Durig, J. R.; Shen, S.; Zhao, W.; Zhou, L. *Chem. Phys.* **1996**, *213*, 165.

(33) Durig, J. R.; Shen, S. *Spectrochim. Acta* **2000**, *56A*, 2545.

(34) Durig, J. R.; Shen, S.; Zhu, X.; Wurrey, C. J. *J. Mol. Struct.* **1999**, *485*, 501.

(35) Durig, J. R.; Zhu, X.; Shen, S. *J. Mol. Struct.* **2001**, *570*, 1.

(36) Guirgis, G. A.; Zhu, X.; Heldrich, F. J.; Wright, M. J.; Durig, J. R. *Phys. Chem. Chem. Phys.* (in press).

(37) Zeisberger, E.; Botskor, I. *J. Mol. Struct.* **1983**, *97*, 323.

(38) Heise, H. M.; Lutz, H.; Dreizler, H. *Z. Naturforsch.* **1974**, *29a*, 1345.

(39) Le Guennec, M.; Wlodarozak, G.; Burie, J.; Demaison, J. *J. Mol. Spectrosc.* **1992**, *154*, 305.

(40) Durig, J. R.; Ng, K. W.; Zheng, C.; Shen, S. *Struct. Chem.* (submitted for publication).

(41) Hirota, E. *J. Chem. Phys.* **1965**, *42*, 2071.